5-2020

Cloning and Expression of Human Synaptosome Associated Protein 29 in E. coli

Logan M. Ryals

The University of Southern Mississippi

Cloning and Expression of Human Synaptosome Associated Protein 29 in *E. coli*

by

Logan Ryals

A Thesis
Submitted to the Honors College of
The University of Southern Mississippi
in Partial Fulfillment
of Honors Requirements

May 2020

Approved by:

_____

Hao Xu, Ph.D., Thesis Adviser,
Associate Professor of Biological Sciences

_____

Jake Schaefer, Ph.D., Director
School of Biological, Environmental, and Earth Sciences

_____

Ellen Weinauer, Ph.D., Dean
Honors College

Abstract

Acting as the chief mediators of vesicular fusion, soluble N-ethylmaleimide-sensitive factor attachment protein receptors (SNAREs) play a role in many intracellular trafficking events by moving opposing membranes into close proximity. One such event takes place in the process of autophagy. A key SNARE involved in autophagy is Synaptosome Associated Protein 29 (SNAP-29), which acts on the autophagosome membrane to promote autophagosome and lysosome fusion. Kaposi's Sarcoma Herpesvirus (KSHV) proteins ORF33 and ORF38 were demonstrated to interact with SNAP-29. The exact mechanism of this interaction is yet to be elucidated but it is hypothesized that these interactions allow KSHV to modulate mast cell autophagy to sustain viral replication. Mast cell degranulation was also demonstrated to be increased upon exposure to KSHV, which might increase tumor progression and viral replication in Kaposi's Sarcoma. To fully characterize the interaction between SNAP29 and KSHV proteins, a recombinant pMBP-parallel-1 expression vector containing human SNAP-29 cDNA was generated. PCR was utilized to amplify SNAP-29 cDNA and insert restriction enzyme sites. Restriction digestion and subsequent ligation were carried out to generate the recombinant pMBP-parallel-1-SNAP-29 construct. This construct was confirmed by sequencing and then used to transform Rosetta 2 (DE3) *E. coli* cells. These cells were then induced by IPTG to express the SNAP-29 protein. SNAP-29 expression was confirmed by the increased intensity of the 71.5 Kda band on an SDS-PAGE gel. Future site-directed mutagenesis of the generated SNAP-29 construct will allow for the identification of the functional domains within SNAP-29 that interact with the ORF33/38 complex through lipid-mixing assays. It is anticipated that these studies may reveal potential therapeutic targets for Kaposi's Sarcoma.

Keywords: SNARE, mast cell, Herpesvirus, Kaposi, autophagy, membranes

Acknowledgements

I would like to thank my thesis advisor, Hao Xu, for providing me with the tools and knowledge necessary for the completion of this project. Furthermore, I am thankful for your patience and understanding throughout the entirety of my time working in the Xu lab. Working in the Xu lab has taught me a great deal about the principles of research, experimental design, and the value of hard work and persistence.

Additionally, I would like to thank Pratikshya Adhikari for her patience and kindness while teaching me lab methods and protocols during my time at the Xu lab. Your input has been invaluable, and I have learned so much about research from you. I would also like to thank Tolulope Ayo for her input and advice throughout the duration of this project.

I would like to thank a fellow undergraduate researcher, Taylor Gore, for his constant support and friendship during our time at the Xu lab. I wish the best of luck to you during your future endeavors.

Lastly, I would like to thank the Mississippi IDeA Network of Biomedical Research Excellence for the contribution of the NanoDrop and gel photoimager which were used throughout this project.

Table of Contents

List of Tables ..... **Error! Bookmark not defined.**ii

List of Figures ix

List of Abbreviations x

Chapter 1: Introduction 1

1.1: Role of Mast Cells as Inflammatory Mediators 1

1.2: Role of SNARE Proteins in Mast Cell Degranulation 3

1.3: SNAP-29 Participates in Augophagolysosome Formation 5

1.4: Mast Cells Are Implicated in the Pathobiology of Kaposi's Sarcoma 6

1.5: Hypothesis 9

Chapter 2: Materials and Methods 10

2.1: Experimental Strategy 10

2.2: Insert and Vector Information 10

2.3: Cloning Oligoprimer Design 11

2.4: PCR 12

2.5: PCR Product Purification 13

2.6: Restriction Digestion 14

2.7: Gel Electrophoresis 15

2.8: Gel Purification 16

2.9: Ligation Reaction 17

2.10: Prepearation of LB Agar With Selective Antibiotics 18

2.11: Transformation of NovaBlue Cells 18

2.12: Streaking Colonies 19

2.13: Culture Inoculation 19

2.14: Plasmid Isolation..... 20

2.15: Plasmid DNA Sequencing 21

2.16: Transformation of Rosetta Expression Cells 21

2.17: Small-scale Protein Indcution..... 22

2.18: SDS-PAGE 23

Chapter 3: Results..... 24

3.1: Amplification of SNAP-29 cDNA..... 24

3.2: Restriction Double Digestion..... 25

3.3: Transformation of NovaBlue Cells..... 27

3.4: Isolated Plasmid Screening..... 28

3.5: Sequencing Confirmation of Isolated Plasmids..... 30

3.6: SNAP-29 Expression 32

Chapter 4: Discussion 35

References..... 38

List of Tables

Table 1: Designed Cloning Primers 12

Table 2: Components of PCR Mixture 12

Table 3: Components of Restriction Digestion Mixtures ..... .15

Table 4: Components of Ligation Reactions 17

Table 5: Sequencing Primer Information 21

Table 6: Gel Purification Results 26

Table 7: Plasmid Isolation Results 29

List of Figures

Figure 1: Schematic of IgE Dependent Mast Cell Degranulation 3

Figure 2: Schematic of SNARE Mediated Membrane Fusion..... 5

Figure 3: Role of Mast Cells in Perpetuation of KS 8

Figure 4: pMBP-parallel-1 Vector Map..... 11

Figure 5: SNAP-29 PCR Program 13

Figure 6: SNAP-29 PCR Product 24

Figure 7: Restriction Digestion Products..... 26

Figure 8: pMBP-parallel-1-SNAP-29 Isolate Screening 28

Figure 9: pMBP-parallel-1-SNAP-29 Isolate Screening 29

Figure 10: pMBP-parallel-1-SNAP-29 Isolate Sequencing Confirmation 31

Figure 11: pMBP-parallel-1-SNAP-29 Isolates Confirmed to be In-frame..... 32

Figure 12: Expression of pMBP-parallel-1-SNAP-29 in Rosetta 2 *E. coli* Cells 34

List of Abbreviations

AND	Anaphylactic Degranulation
CAT	Chloramphenicol Acetyltransferase
EC	Endothelial Cell
IgE	Immunoglobulin E
IPTG	Isopropyl β-d-1-thiogalactopyranoside
KS	Kaposi's Sarcoma
KSHV	Kaposi's Sarcoma Herpesvirus
LB	Lytic Broth
MBP	Maltose Binding Protein
MC	Mast Cell
NSF	N-ethylmaleimide-sensitive factor
OD_{600}	Optical Density at 600 nm wavelength
PCR	Polymerase Chain Reaction
PMD	Piecemeal Degranulation
PMSF	Phenylmethylsulfonyl Fluoride
rSAP	Shrimp Alkaline Phosphatase
SDS PAGE	Sodium Dodecyl Sulfate Polyacrylamide Gel Electrophoresis
SNARE	Soluble NSF Attachment Protein Receptor
SNAP-29	Synaptosome Associated Protein 29
STX	Syntaxin
VAMP	Vesicle Associated Membrane Protein

Chapter 1: Introduction

1.1: Role of Mast Cells as Inflammatory Mediators

Mast cells (MCs) are a specialized class of white blood cells that carry out an important role in the human body by responding to pathogens and mediating the release of a variety of compounds upon antigen exposure (Urb & Sheppard, 2012). Mast cells are known to release proinflammatory modulators as well as proteases that cleave inflammatory cytokines (Piliponsky, et al., 2012; Waern, et al., 2012). The release of these contents allows mast cells to maintain the homeostatic balance of both proinflammatory and anti-inflammatory mediators (Xu & Sugita, 2018).

Localized primarily in human tissues such as mucosal linings and the connective tissue lining blood vessels (Gilfillan & Beaven, 2011; Moon, et al., 2010), mast cells are activated to release active compounds stored in endocytic vesicles, called granules. This activation is initiated by many ligand-receptor interactions including immunoglobulin E (IgE) and pathogen-associated molecular pattern recognition receptor stimulation (Shelburne & Abraham, 2011), inducing signaling cascades to eventually release a variety of mediator molecules (Xu & Sugita, 2018). The actions of these mediators are associated with activating both native and adaptive immune responses. These actions allow mast cells and the granular contents they release to serve as integral regulators in ensuring the proper functionality of the immune system (Gilfillan & Beaven, 2011). Mast cell mediators broadly fall under two main classes: preformed mediators (including histamine and β-hexosaminidase) and newly synthesized mediators (including cytokines and chemokines). These mediators are released through either regulated or constitutive exocytosis mechanisms (Xu & Sugita, 2018).

The release of contents stored in MC granules is further described as anaphylactic degranulation (AND) or piecemeal degranulation (PMD). Anaphylactic degranulation refers to the homotypical fusion of granules with one another and the heterotypical fusion of granules with the cytoplasmic membrane to result in complete release of vesicle contents. Piecemeal degranulation refers to the transport of granule contents into smaller vesicles before heterotypical fusion (Xu & Sugita, 2018). The variation in mechanisms used to release granule contents adds complexity to the exocytic pathways utilized by MCs and complicates the current understanding of the modes by which these pathways are regulated.

The dysregulation of MC degranulation plays a key role in the pathobiology of a variety of human diseases including cancer, autoimmunity, cardiovascular disease, and allergic inflammation (Xu & Sugita, 2018). The pathobiology of allergic inflammation is directly propagated by the binding of IgE to IgE receptors found on the MC plasma membrane to initiate overactive degranulation. These degranulation events are characterized by a massive release of proinflammatory mediators, including histamine, to result in the production of the acute phase allergic reaction in hypersensitivity responses, such as asthma (Lei, Gregory, Nilsson, & Adner, 2013). This process first involves the production of secreted IgE by plasma cells under the direction of Th2 released cytokines during the type 1 hypersensitivity reaction. This cytokine release is followed by subsequent binding of IgE to the Fc receptor specific to IgE, FcεRI, found on the cell membrane of mast cells. This process is known as IgE sensitization. Next, an antigen or allergen will bind to IgE and initiate receptor aggregation and subsequent cross-linking of IgE molecules (Gilfillan & Beaven, 2011). The formation of this cross-linkage initiates

the influx of Ca^{2+} through inositol triphosphate intracellular signaling to initiate a cascade within the MC (Kraft, & Kinet, 2007). This multistep signaling cascade ends in the eventual release of MC granular contents, including histamine and interleukins, which perform a variety of actions within the body, including promoting inflammation (Gilfillan & Beaven, 2011) (Fig.1). The prevalence of MC degranulation in hypersensitivity-related diseases including asthma has prompted the detailed characterization of the specific downstream protein interaction cascade that gives rise to MC degranulation.

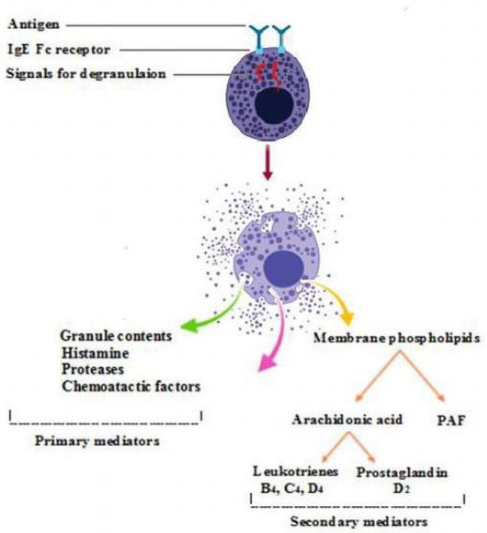

Figure 1: Schematic of IgE Dependent Mast Cell Degranulation
IgE sensitization is the first step of the IgE dependent MC degranulation pathway and is dependent on the binding of IgE produced by plasma cells to FcεRI situated on the MC membrane facing the extracellular space. Next, the binding of an antigen or allergen stimulates the cross-linking of IgE, which stimulates a signaling cascade within the cell. This results in degranulation, which leads to the release of a variety of mediator molecules. Retrieved from Arora, P., & Ansari, S. H. (2019). Role of Various Mediators in Inflammation of Asthmatic Airways. In *Asthma-Biological Evidences*. IntechOpen.

1.2: Role of SNARE Proteins in Mast Cell Degranulation

In mast cell IgE dependent degranulation, SNARE proteins (Soluble NSF Factor Receptors) are activated in a calcium dependent fashion and catalyze the fusion of vesicle and plasma membranes to result in MC degranulation (Nishida, et al., 2005). These proteins are a conserved group of eukaryotic membrane bound proteins that are found on

both vesicular and plasma membranes associated with the fusion of membranes in a variety of biological processes. Opposing SNARE partners interact to give rise to a four-helical bundle known as the trans-SNARE complex. The formation of the trans-SNARE complex typically involves the interaction between one R-SNARE and either two or three Q-SNAREs. The distinction between R and Q refers to whether an arginine (R) or glutamine (Q) side chain is contributed to the helical bundle. Additionally, Q-SNAREs are further classified as either Qa-SNAREs which contribute one helix to the four-helical bundle or Qbc-SNAREs which contribute two helices to the four-helical bundle. Contrastingly, R-SNAREs always contribute one helix to the four-helical bundle (Fasshauer, Sutton, Brunger, & Jahn, 1998; Kloepper, Kienle, & Fasshauer, 2007). Membrane fusion events along the secretory pathways and the endocytic pathways require the interaction of three Q-SNAREs on one membrane and one R-SNARE on the other (Fasshauer, et al., 1998).

Although they are the principal drivers of membrane fusion, SNAREs rely on other protein partners for the successive steps of docking, priming, and lipid fusion to occur. Docking is carried out by a protein called exocyst and involves the trafficking of vesicles to the target membrane (Toonen, et al., 2006). Next, Qa- and Qbc-SNAREs interact to form a resting cis-SNARE complex on the plasma membrane. Munc13, N-ethylmaleimide-sensitive factor (NSF), and other factors interact with the SNARE machinery and partially assemble the Q-SNAREs and R-SNAREs into the trans-SNARE complex, priming the vesicle and target membrane (Toonen, et al., 2006). Lastly, IgE stimulation results in the influx of calcium ions into the mast cell. Synaptotagmin is activated upon calcium binding to assist the trans-SNARE complex in bringing the

opposing membranes into close proximity, permitting fusion of the membranes and resulting in exocytosis.

The specific Q-SNAREs contributing to mast cell degranulation have been identified as SNAP-23 and Syntaxin (STX) 2, 3, 4, and 6. The specific R-SNAREs contributing to mast cell degranulation have been identified as Vesicle associated membrane protein (VAMP) 2, 3, 4, 7, and 8 (Lorentz, Baumann, Vitte, & Blank, 2012). The interaction between SNARE proteins along with the interaction of SNARE accessory proteins, including Munc18, Munc13, and Rab GTPases, gives rise to mast cell degranulation upon mast cell activation (Lorentz, et al., 2012) (Fig. 2).

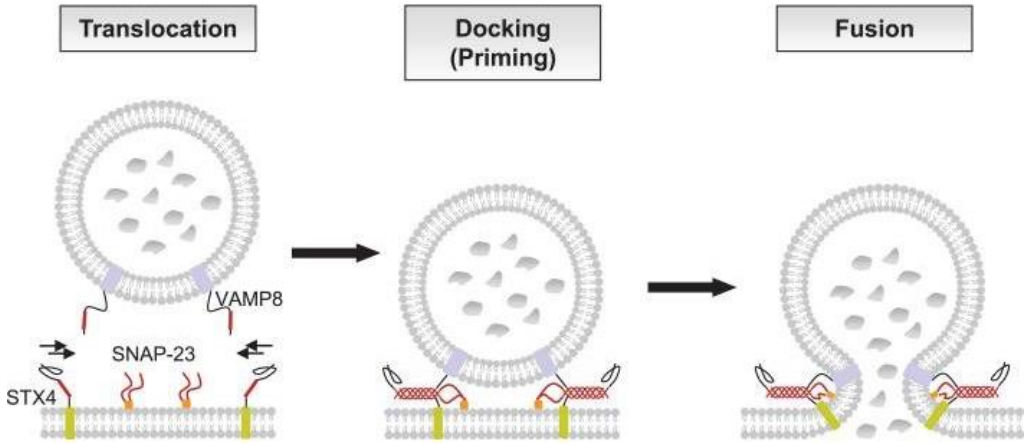

Figure 2: Schematic of SNARE Mediated Membrane Fusion VAMP8, the R-SNARE, is brought into close proximity to the cis-SNARE complex of Qa-SNARE STX4 and Qbc-SNARE SNAP-23 during the translocation step. The trans-SNARE complex between the Q-SNAREs and R-SNARE is then formed in the priming step leading to fusion of the two membranes which results in exocytosis. Adapted from Lorentz, A., Baumann, A., Vitte, J., & Blank, U. (2012). The SNARE machinery in mast cell secretion. *Frontiers in immunology*, *3*, 143.

1.3: SNAP-29 Participates in Autophagolysosome Formation

Although not implicated in the well-described mechanism of mast cell degranulation, SNAP-29 is a Qbc-SNARE found in mast cells that has been identified as a key component in autophagosome-lysosome fusion in Drosophila (Takáts, et al., 2018).

Within this model, SNAP-29 and STX-17 have been demonstrated to form a trans-SNARE complex with R-SNARE VAMP-8 to promote the fusion of the autophagosome and lysosome vesicles (Takáts, et al., 2018).

Autophagosome-lysosome fusion is an event that takes place during the process of autophagy. Autophagy is a mechanism that is utilized by eukaryotic cells to recycle damaged or worn organelles and to liberate nutrients during a state of cellular stress (Karanasios & Ktistakis, 2016). This process is also carried out by the cell to combat intracellular pathogens by trafficking them to lysosomes for degradation (Levine, 2005). As a result, many families of viruses have been shown to exploit the autophagosome-lysosome fusion process to aid viral replication and maturation within host cells (Richards & Jackson, 2012). For example, Picornavirus EV-D68 is a respiratory virus that interacts with SNAP-29 to signal the autophagic pathway. This interaction also promotes viral replication during the early stages of replication. The Qbc-SNARE is subsequently cleaved during cellular exit to prevent autophagolysosome formation in H1HeLa cells (Corona, Saulsbery, Velazquez, & Jackson, 2018). The EV-D68 C3 protein was demonstrated to perform the proteolytic cleavage of SNAP-29 at Q161 to prevent the fusion of the lysosome and autophagosome, thus favoring viral replication in late stages of viral replication (Corona, et al., 2018).

1.4: Mast Cells Are Implicated in the Pathobiology of Kaposi's Sarcoma

Mast cells have also been implicated in the pathogenesis of Herpesviruses associated diseases including Kaposi's Sarcoma (KS) (Ayers, et al., 2018; Aoki, et al., 2013). Kaposi's Sarcoma is described as a hemorrhagic condition of endothelial cells (ECs) caused by the infection of Kaposi's Sarcoma Herpesvirus (KSHV). The tumors

that arise from KSHV infection are characterized by invading leukocytes as well as proliferating spindle-shaped ECs, which accumulate (Ganem, 2006). However, these ECs have been demonstrated to grow in culture without producing viral progeny, indicating that infected ECs envelop latent virus and are not able to harbor infectious KSHV (Grundhoff, & Ganem, 2004). In contrast, MCs have been observed to play a large role in perpetuating KSHV, as these cells have been shown to support viral gene expression and sustain an infectious viral load for long durations (Ayers, et al., 2018). Furthermore, in addition to serving as a potential reservoir of KSHV, mast cells are known to increase degranulation upon interaction with expressed viral proteins (Ayers, et al., 2018). Harboring KSHV in MCs is thought to result in the long-term propagation of the active viral infection in ECs (Ayers, et al., 2018). The increased activation of MCs and subsequent abundant release of heparin and histamines is implicated in edema and increased tumorigenesis and hemorrhaging of closely associated blood vessels (Ayers, et al., 2018). These outcomes are consistent with the histologic features presented in KS and the known effects of these mediators (Ayers, et al., 2018). Therefore, it is postulated that the combination of MC activation along with the release of viral progeny from these infected cells results in the progression of KS tumors (Fig. 3).

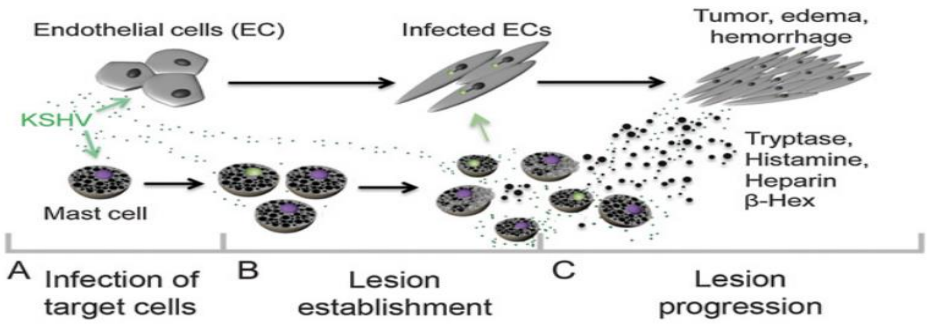

Figure 3: Role of Mast Cells in Perpetuation of KS Mast cells were observed to maintain a high viral titer throughout KSHV infection. These cells were also shown to be activated under infection conditions to release mediators associated with tumor progression. Adapted from Ayers, L. W., Barbachano-Guerrero, A., McAllister, S. C., Ritchie, J. A., Asiago-Reddy, E., Bartlett, L. C., ... & King, C. A. (2018). Mast cell activation and KSHV infection in Kaposi sarcoma. *Clinical Cancer Research*, *24*(20), 5085-5097

Recently, conserved Herpesviridae proteins ORF33 and ORF38 have been linked to the replication and maturation process of KSHV (Wu, et al., 2016). Both of these proteins were found to be expressed in the late lytic cycle and to be retained in mature viruses as tegument proteins. The ORF38 protein was shown to colocalize with Golgi and early endosome vesicles. Interaction between ORF38 and ORF33 was found to be crucial for optimal production of progeny virions through the triggered expression of RTA, thus inducing lytic gene expression (Wu, et al., 2016). The KS protein ORF33 was found to localize on cytosolic vesicles once bound by ORF38. Importantly, these KSHV tegument proteins have been demonstrated to carry out interactions with Qbc-SNARE protein SNAP-29 (Xu, unpublished). However, the precise mechanism of these interactions has yet to be examined. Determining the mechanism by which these interactions take place may unveil therapeutic targets which can be exploited to prevent the perpetuation of KS by mast cells. Targeting the protein domains involved in these interactions could

effectively reduce the progression of KS tumors and allow for more efficacious treatment when combined with classical therapeutic strategies.

1.5: Hypothesis

It has previously been shown that, once KSHV enters the MC, tegument proteins ORF38 and ORF33 interact with SNAP-29. It is hypothesized here that ORF 33/38 may act in a manner similar to EV-D68 protein C3 and cleave SNAP-29 between its two SNARE binding motifs to prevent formation of the autophagolysosome. Furthermore, it is thought that this mode of interaction with autophagolysosomal fusion machinery would enable MCs to serve as reservoirs of viral progeny during KSHV infection.

In order to test this hypothesis, SNAP-29 was cloned into the *E. coli* expression vector pMBP-parallel-1 and expressed in *E. coli* Rosetta 2 (DE3) cell lines. The generation of this construct will allow future studies to be conducted to dissect interactions between KSHV proteins and SNAP-29. In those studies, lipid fusion assays will be carried out, which will employ the principles of mutational analysis to elucidate which SNAP-29 domains interact with KSHV tegument proteins ORF33/38. Determining the interaction of these participating domains may identify drug targets within SNAP-29, which may be exploited to enhance autophagosome-lysosome fusion and promote MC clearance of the virus.

Chapter 2: Methods and Materials

2.1 Experimental Strategy

A classical cloning approach was utilized in order to produce the recombinant SNAP-29 construct and subsequently express the protein. Firstly, SNAP-29 cDNA was amplified and restriction enzyme sites were inserted using a standardized protocol. Both pMBP-parallel-1 and the amplified SNAP-29 cDNA were digested with BamHI and XbaI. Ligation was then carried out and the construct was used to transform NovaBlue *E. coli*. Next, plasmid DNA was isolated from these cells and subsequently analyzed by DNA sequencing. The recombinant plasmid was then used to transform Rosetta 2 (DE3) *E. coli*, which were then induced to express SNAP-29. Expression of the protein was analyzed via sodium dodecyl sulfate polyacrylamide gel electrophoresis (SDS-PAGE).

2.2 cDNA and Vector Information

The human SNAP-29 cDNA was obtained from the pMRXIP GFP-SNAP-29 plasmid from Noboru Mizushima (addgene plasmid #45923). The pMBP-parallel-1 vector was obtained from the HXB_OC21 strain cultured in the C992 derivative of DH5 alpha *E. coli* obtained from Kevin Collins of The Geisel School of Medicine at Dartmouth. A vector map of pMBP-parallel-1 is detailed in Fig. 4.

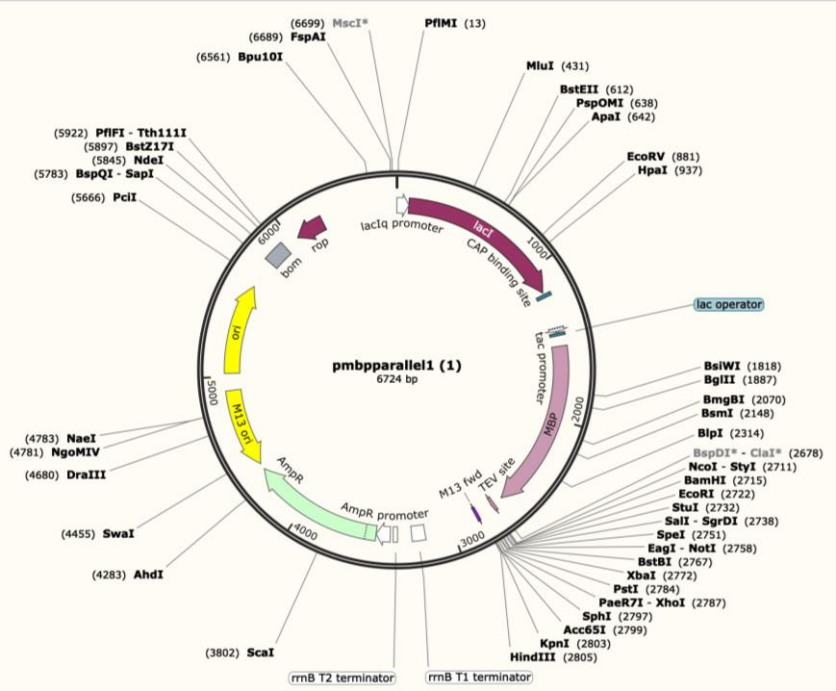

Figure 4: pMBP-parallel-1 Vector Map AmpR refers to the ampicillin resistance gene and MBP refers to the maltose binding domain of the fusion protein product. The nucleotide sequence for pMBP-parallel-1 was obtained from NCBI and mapped using SnapGene.

2.3 Cloning Oligoprimer Design

To insert SNAP-29 into the pMBP-parallel-1 vector, cloning primers had to be designed. First, the sequence of SNAP-29 was input into the online program NEBcutter 2.0 in order to determine the restriction enzyme sites to include in the designed primers. The selection of BamHI and XhoI was made on the basis that these two cut sites were found within the multiple cloning site of the pMBP-parallel-1 vector but not within the sequence of SNAP-29. BamHI was selected for the 5’ oligoprimer and XhoI was selected for the 3’ oligoprimer, as these cut sites lie on the 5’ and 3’ end of the pMBP-parallel-1 multiple cloning site, respectively. The designed primers are detailed in Table 1. Capital letters denote restriction enzyme sites. The HXO_E14 primer contains a restriction site for BAM HI while HXO_E15 contains a restriction site for XhoI. An extra guanosine

nucleotide was included in primer HXO_E14 so that SNAP-29 would be in frame with MBP and the TEV site upon ligation. These oligoprimers were custom made by Sigma Aldrich.

Table 1: Designed Cloning Primers

Oligoprimer Name	Nucleotide Sequence	GC Content	Tm	Directionality
HXO_E14	5'-atgGGATCCgatgtcagcttaccctaaaagc-3'	48%	73°C	Forward
HXO_E15	5'-ccgCTCGAGtcagagttgtcgaacttttc-3'	52%	73°C	Reverse

Capital letters denote restriction enzyme sites.

2.4 PCR

The SNAP-29 cDNA was amplified via polymerase chain reaction (PCR) using the designed cloning primers and the pMRXIP GFP-SNAP-29 plasmid as the template. The PCR mixture components were added to a PCR tube on ice and mixed by spinning. The contents and volumes aliquoted into the PCR mixture are detailed in Table 2. A micropipette was used to add sterile Millipore water, 10X Pfu Polymerase Buffer, 10 µM Primer HXO_E14, 10 µM Primer HXO_E15, 10 µM dNTPs, Pfu DNA Polymerase, and template SNAP-29. The PCR mixture was then subjected to the PCR program outlined in Fig. 5. After the conclusion of the PCR program, the PCR product was stored at -20ºC.

Table 2: Components of PCR Mixture

Component	Volume
10X Pfu Polymerase Buffer	5µL
Tempelate SNAP29 (295.5ng/µL)	0.5µL
10µM FWD Primer (HXO_E14)	1µL
10µM RVS Primer (HXO_E15)	1µL
10µM dNTPs	1µL
Pfu DNA Polymerase (G Bioscience)	1µL
Sterile Millipore Water	40.5µL

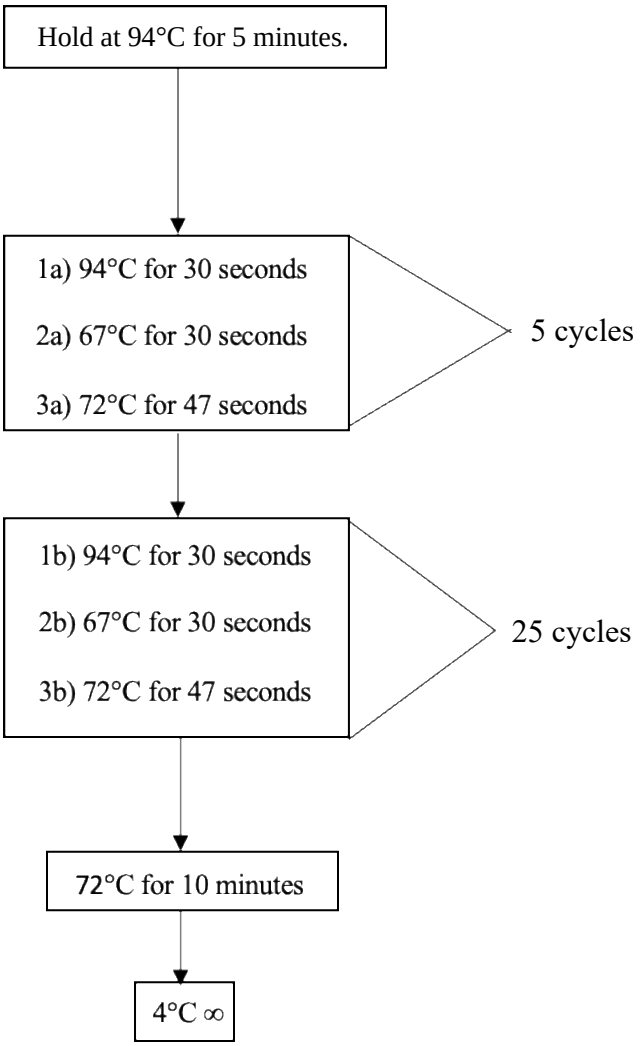

Figure 5: SNAP-29 PCR Program The SNAP-29 cDNA was amplified using a standardized PCR protocol. The annealing temperature for the first five cycles was lowered as to accommodate the difference in annealing temperatures between the two oligoprimers.

2.5 PCR Product Purification

Following PCR, the amplified SNAP-29 cDNA containing a 5' BamHI and a 3' XbaI restriction site was purified using the QIAquick PCR Purification Kit to remove DNA polymerase, residual primers, and any salts from the polymerase buffer. A micropipette was used to add 250 µL of Buffer PB and 50 µL of the PCR product mixture into a sterile 1.5 mL microfuge tube. This solution was mixed by spinning and transferred to a QIA

spin column that was placed inside a collection tube. The sample was then centrifuged at 17,000 xg for one minute. The flow-through was discarded and the column was replaced inside the collection tube. A micropipette was used to add 750 µL of Buffer PE to the spin column to wash the sample. The sample was again centrifuged at 17,000 xg for one minute. The flow-through was discarded and the column was again replaced inside the collection tube. This was repeated twice more for a total of three centrifugations after adding Buffer PE. The spin column was then placed into a sterile 1.5 mL microfuge tube. A micropipette was used to add 30 µL of sterile Millipore water to the center of the spin column membrane. The spin column was held at room temperature for one minute before centrifugation at 17,000 xg to elute the purified DNA. The absorbance of the eluted DNA was then measured by a Nanodrop spectrophotometer, using sterile Millipore water as the blank. The spectrophotometer was used to determine the concentration of DNA in the sample as well as purity denoted by absorbance values. A micropipette was used to load 1 µL of the eluted DNA into the spectrophotometer, which provided the concentration of the sample in ng/µL and absorbance ratios as A260/230 and A260/280. The purified PCR product was then stored at -20 ºC.

2.6 Restriction Digestion

To insert SNAP-29 into the pMBP-parallel-1 vector, both the cDNA and the vector were digested by restriction enzymes BamHI and XbaI. The contents of the restriction digest mixtures, which were prepared on ice, are detailed in Table 3. The reactions were then mixed, placed in a water bath and incubated at 37 ºC for 3 h. The reactions were then mixed by spinning and placed on a heat block to incubate at 65 ºC for 20 min to stop the restriction digestion reaction. The SNAP-29 double digest was then stored at -20 ºC. A

micropipette was then used to add 1 µL of 1,000 U/mL shrimp alkaline phosphatase (rSAP) (supplied by NEB) to double digested pMBP-parallel-1 to dephosphorylate the 5' end of the linearized vector. The rSAP reaction was then mixed and placed into a water bath at 37 ºC for one hour. The rSAP reaction mixture was then mixed by spinning and placed on a heat block to incubate at 65 ºC for 20 minutes to stop the reaction. Following inactivation, the vector was then stored at -20 ºC.

Table 3: Components of Restriction Digestion Mixtures

SNAP 29 Double Digest		pMBP-parallel-1 Double Digest	
Component	Volume	Component	Volume
PCR Purified SNAP29	27µL	pMBP-parallel-1	25µL
10X NEB CutSmart Buffer	5µL	10X NEB CutSmart Buffer	5µL
BamHI HF	1µL	BamHI HF	1µL
XhoI	1µL	XhoI	1µL
Sterile Millipore Water	16µL	Sterile Millipore Water	18µL
Total Volume:	50µL	Total Volume:	50µL

2.7 Gel Electrophoresis

To separate the digested fragments of interest, both the digested SNAP-29 insert and the digested pMBP-parallel-1 vector were subjected to electrophoresis on an agarose gel. A 0.7% agarose gel was prepared by dissolving 350 mg of agarose in 50 mL of 0.5X TBE buffer. The 0.5X TBE buffer was diluted tenfold from a 1 L 5X TBE (pH 8.3) stock solution containing 54 g Tris base, 27.5 g boric acid, and 20 mL 0.5 M EDTA (pH 5) dissolved in sterile Millipore water. The agarose and buffer were added to a 250 mL Erlenmeyer flask and heated by microwaving for three 30 second intervals. The solution was mixed in-between each interval until the solution became clear. The molten agarose solution was then poured into a gel casting apparatus which contained a gel tray with a comb inserted. The gel was kept at room temperature for 45 minutes to solidify. The

solidified gel inside of the gel tray was then transferred into a gel electrophoresis tank filled with 0.5X TBE buffer. The tank was then further filled with 0.5X TBE buffer until the gel became completely submerged. Samples were then loaded into each well along with 2 µL of 18X Gel Red and autoclaved Millipore water to equal 10 µL of each loaded sample. The 10,000X Gel Red stock (Biotium) was diluted to 100X in Millipore water. This 100X solution was then diluted with 6X purple loading dye (NEB) to make the 18X Gel Red solution. The top was then placed onto the gel electrophoresis chamber and the gel was electrophoresed at 80 V for 60 minutes at varying amplitude.

2.8 Gel Purification

Following gel electrophoresis, the desired bands were then purified. This procedure was carried out using the QIAquick Gel Extraction Kit. A clean and sharp scalpel was used to excise the desired bands (0.7 kb for SNAP-29 and 6.7 kb for pMBP-parallel-1). These excised bands were then added to separate sterile microfuge tubes and placed on a microscale to weigh the fragments. The fragment weights were then recorded. A micropipette was then used to add three volumes of Buffer QG to one gel volume in the microfuge tube. The two microfuge tubes were then incubated at 50 ºC inside of a heat block. The microfuge tubes were vortexed every two minutes for the duration of 10 minutes until the gel fragments were dissolved. A micropipette was then used to add one gel volume of isopropanol to each microfuge tube before mixing both tubes by spinning. Two spin columns were then placed into two 2 mL tubes labeled SNAP-29 and pMBP-parallel-1. A micropipette was used to transfer each sample into the appropriate spin column. Next, a micropipette was used to add 750 µL of Buffer PE to each column. Both columns were then centrifuged at 17,000 xg for one minute and the flow-through was

discarded. The columns were centrifuged two additional times at 17,000 xg for one minute to rid the samples of residual buffer. Each column was placed into a clean 1.5 mL microcentrifuge tube labeled SNAP-29 and pMBP-parallel-1. A micropipette was used to add 30 µL of sterile Millipore water to each column. Each column was centrifuged at 17,000 xg for one minute. Each eluted sample was loaded onto a NanoDrop spectrophotometer to determine the absorbance values and concentration of each sample.

2.9 Ligation Reaction

Following gel purification, the purified SNAP-29 and pMBP-parallel products were subjected to a ligation reaction to insert SNAP-29 into the vector. The components of the ligation mixture were added via a micropipette into a sterile PCR tube on ice. A control mixture was also included which lacked the SNAP-29 insert to assay vector self-reannealing. A micropipette was used to add sterile Millipore water, 10X T4 DNA Ligase Buffer (NEB), 16.8 ng/µL pMBP-parallel-1, T4 DNA Ligase (NEB), and 27.4 ng/µL SNAP-29. The components of each mixture are detailed in Table 4. Once these components were added, both sample solutions were mixed by spinning. Both mixtures were then incubated at 17 ºC in a thermocycler for 16 hours. The ligation products were stored at -20 ºC.

Table 4: Components of Ligation Reactions

Ligation Reaction		Vector Only Control	
Component	Volume	Component	Volume
Sterile Millipore Water	10.5µL	Sterile Millipore Water	11µL
10X T4 Ligase Buffer	1.5µL	T4 Ligase Buffer	1.5µL
16.8ng/µL pMBP-parallel-1	1.5µL	16.8ng/µL pMBP-parallel-1	1.5µL
T4 DNA Ligase	1µL	T4 DNA Ligase	1µL
27.4ng/µL SNAP29	0.5µL	27.4ng/µL SNAP29	-
Total Volume:	15µL	Total Volume:	15µL

2.10 Preparation of LB Plates with Selective Antibiotics

Selective lytic broth (LB) plates were prepared to isolate transformed colonies. Ampicillin at a concentration of 100 µg/mL was used to isolate transformed cells since the pMBP-parallel-1 vector contains an ampicillin resistance gene.

Firstly, 6 g of Bacto agar was measured and placed into a sterilized 500 mL bottle. A graduated cylinder was used to add 300 mL of freshly prepared LB media into the 500 mL bottle. This bottle was then labeled and autoclaved through a liquid 20 cycle. The bottle of dissolved LB agar was allowed to cool at room temperature. Once the solution had cooled, a micropipette was used to add 300 µL of 100 mg/mL ampicillin to the LB agar to yield 300 mL of LB agar containing 100 µg/mL ampicillin. Approximately 20 mL of this solution was poured into each petri dish over a Bunsen burner. These plates were held at room temperature until they became solidified. The plates were labeled AMP 100 and stored at 4 ºC.

2.11 Transformation of NovaBlue Cells

Competent NovaBlue *E. coli* were transformed using the ligation mixture as well as the vector only mixture to serve as a control. First, competent NovaBlue *E. coli* cells were allowed to thaw on ice. These cells were mixed by pipetting up and down with a micropipette. A micropipette was then used to mix 2.0 µL of each ligation mixture with 20 µL of competent cells in separate clean 1.5 mL microfuge tubes. The competent cells were mixed together with the ligation mixtures by gently tapping the wall of the microfuge tubes. The cells and ligation mixture were then kept on ice for 45 minutes. Next, the cells were placed on a heat block set at 42 ºC for 30 seconds to heat shock the cells. A micropipette was used to add 100 µL of SOC medium to each microfuge tube.

The medium was added over a Bunsen burner to decrease the risk of contamination. The entire volume of each microfuge tube was added to 100 µg/mL ampicillin LB agar plates. Five autoclaved glass beads were then added to each plate. The plates were rotated horizontally for 15 seconds to create a bacterial lawn. Next, the plates were placed in a 37 ºC incubator for 20 minutes. The plates were then flipped upside down and stored in the 37 ºC incubator overnight.

2.12 Streaking Colonies

Transformed colonies were streaked onto new plates to ensure that pure colonies were obtained. The 100 µg/mL ampicillin LB agar plate containing transformed colonies was retrieved from the 37 ºC incubator. Four fresh 100 µg/mL ampicillin LB agar plates were retrieved from 4 ºC storage and allowed to warm at room temperature. Next, an individual colony was picked from the agar plate containing transformed colonies using a wooden inoculation wand. This process was carried out over a Bunsen burner to decrease the risk of contamination. This colony was streaked over one quarter of a fresh 100 µg/mL ampicillin LB agar plate. This wand was discarded, and a fresh wand was used to streak the remaining three quarters of the plate. This process was carried out for the four individual colonies. Each streaked plate was held at 37 ºC overnight in the incubator.

2.13 Overnight Culture Inoculation

The four streaked plates were retrieved from the 37 ºC incubator and placed at room temperature. Over a Bunsen burner, 5 µL of 100 mg/mL ampicillin was added to four test tubes, each containing 5 mL of LB medium to prepare 100 µg/mL ampicillin LB. A single colony was picked from each streaked plate using a clean inoculation wand and

placed into a test tube containing 100 µg/mL ampicillin LB. These inoculated cultures were placed in a 37 ºC rotating shaking incubator overnight.

2.14 Plasmid DNA Isolation

The overnight cultures were used to isolate the plasmid DNA using the QIA Miniprep kit. The four overnight cultures were placed on ice and vortexed to resuspend cells at the bottom of the test tube. A serological pipette was used to add 1.5 mL of each culture to a microfuge tube. These tubes were centrifuged at 17,900 xg for one minute. The supernatant was decanted before adding an additional 1.5 mL of the culture to the tube. The samples were again centrifuged at 17,000 xg for one minute. The supernatant was, again, decanted and the pellet was vortexed until all sediment was resuspended. A micropipette was used to add 250 µL of buffer P1 as well as to add 250 µL of buffer P2 to each tube. The tubes were inverted ten times and the solution was noted to become clear. A micropipette was used to add 350 µL of buffer N3 to each tube. The tubes were again inverted ten times before centrifuging at 17,000 xg for 10 minutes at 4ºC. The supernatant was removed from each tube and added to a QIA column which was placed inside of a 1.5 mL microfuge tube. Each tube was centrifuged at 17,000 xg for one minute. The flow through was discarded and a micropipette was used to add 500 µL of buffer PB to each QIA column. Each column was again centrifuged at 17,000 xg for one minute. The flow through was discarded and a micropipette was used to add 750 µL of buffer PE to each QIA column. Each tube was centrifuged at 17,000 xg for one minute. The flow through was then discarded and the columns were centrifuged twice more to remove any residual buffer. Each column was transferred into a clean 1.5 mL microfuge tube. A micropipette was used to add 50 µL of autoclaved Millipore water to each tube.

The tubes were held at room temperature for one minute and then were centrifuged at 13,000 xg for one minute. Each isolated plasmid was loaded onto a NanoDrop spectrophotometer so that the concentration and purity of the sample could be obtained. The samples were then stored at -20 ºC.

2.15 Plasmid DNA Sequencing

To verify that the correct plasmid had been isolated, two plasmids isolated from separate colonies were mailed to Eurofins Genomics for sequencing. The components that were included in each tube were added on ice. A micropipette was used to add 5.9 µL of the isolated plasmid DNA (Table 7), 4 µL of a 1.6 µM pMBP forward primer, and 2.1 µL of autoclaved Millipore water. The sequencing primer details are included in Table 5.

Table 5: Sequencing Primer Information

Oligoprimer Name	Nucleotide Sequence	GC Content	Tm	Directionality
MBP FWD	5'-gcgcagactaattcgagc-3'	56%	56°C	Forward

2.16 Transformation of *E. coli* Rosetta 2 (DE3) Expression Cells

Once the plasmid of interest was verified by sequencing, Rosetta 2 (DE3) expression *E. coli* cells (Novagen) were transformed with the plasmid. Two separate transformation reactions were carried out. One transformation was carried out using SNAP-29 Isolate #1 while the other transformation was carried out using SNAP-29 Isolate #2. Firstly, the cells were thawed on ice and mixed by gently flicking the container. A micropipette was used to transfer 10 µL of competent cells to two sterile 1.5 mL microfuge tubes along with 1 µL of plasmid DNA. The components were mixed by again gently flicking the container. These cells were held on ice for 45 minutes before heat shocking the cells at 42 ºC for 45 seconds. The transformation mixtures were returned to ice for 20 minutes. A

micropipette was then used to add 90 µL of LB medium to the transformation mixtures. The mixtures were placed into an incubator and held at 37 ºC for one hour. Next, the transformation mixtures were plated onto two LB agar plates containing 34 µg/mL chloramphenicol and 100 µg/mL ampicillin. Five sterile glass beads were added to each plate which was then rotated horizontally to spread the bacterial cells across the plate. The plates were placed into an incubator and held at 37 ºC for 20 minutes before flipping the plates and holding them at 37 ºC overnight.

2.17 Small-Scale IPTG Protein Induction

After transformation, a colony was streaked from each transformation plate. A single colony was inoculated from each streak plate into separate tubes containing 5 mL of LB medium with 34 µg/mL chloramphenicol and 100 µg/mL ampicillin. These tubes were incubated at 37 ºC overnight in the rotating shaker. The optical density at 600 nm wavelength (OD_{600}) was measured 17 hours later. Next, a micropipette was used to add 800 µL of the overnight cultures into separate tubes containing 10 mL of fresh LB along with 34 µg/mL chloramphenicol and 100 µg/mL ampicillin to reach OD_{600} = 0.08. These cultures were mixed gently by pipetting and divided into two separate tubes labeled IPTG (+) and IPTG (-). This was done for both overnight cultures meaning there was a total of four tubes. All four of the tubes were held at 37 ºC in the rotating shaker for three hours, until the cultures reached OD_{600} = 0.4. A micropipette was used to add 2.5 µL of 1M Isopropyl β-d-1-thiogalactopyranoside (IPTG) to each IPTG (+) tube to reach 0.5 mM IPTG. Each tube was then returned to the rotating shaker and held at 37 ºC for 4 hours. Next, the OD_{600} was again obtained from each culture. One OD_{mL} was then taken from each culture and placed into a 1.5 mL microfuge tube. These 1 OD_{mL} samples were spun

in a microfuge for one minute at 13,000 xg. The supernatant was then discarded from each sample and the pelleted cells were resuspended in 100 µL of 2X SDS PAGE loading buffer containing 1 mM phenylmethylsulfonyl fluoride (PMSF). Glass beads were added to each resuspended sample before vortexing for one minute. Each sample was boiled at 95 ºC for 5 minutes before storing at -20ºC.

2.18 SDS-PAGE

The IPTG (+) and IPTG (-) samples were analyzed via SDS-PAGE to determine if SNAP-29 expression had been induced. Firstly, a 12% acrylamide gel was made using a standardized protocol. Samples were boiled at 94 ºC for 5 minutes before loading onto the SDS-PAGE gel. Next, 10 µL of each sample was loaded into each well. 1x SDS running buffer was then added into the running tray. Gel electrophoresis was performed at 150 V for one hour with varying current. The gel was immersed in a Coomassie Brilliant Blue R-250 staining solution overnight. The staining solution was then removed, and the gel was immersed in destaining solution for two hours. Lastly, the gel was imaged using a gel photoimager and subsequently analyzed.

Chapter 3: Results

3.1: Amplification of SNAP-29 cDNA

To amplify human SNAP-29 cDNA, a PCR reaction was carried out using the pMRXIP GFP-SNAP-29 template and primers HXO_E14 and HXO_E15 to insert a 5' BamHI cut site and a 3' XhoI cut site into the SNAP-29 cDNA. The PCR product was purified before electrophoresis. The PCR product showed banding at approximately 0.8 Kb, consistent with the expected size of 777 bp for SNAP-29 (Fig. 6). Subsequent PCR purification yielded a concentration of 47.5 ng/µL, an A260/280 value of 1.83, and an A260/230 value of 1.92. Both of the absorbance ratios were nearing 2.0, indicating adequate purity of the sample. The amplification and purification of SNAP-29 cDNA using the designed primers generated cDNA which contained restriction sites for BamHI and XhoI. The insertion of these restriction sites was a crucial step for generating the recombinant plasmid as it allowed for complementary single-stranded segments to be generated in both SNAP-29 and pMBP-parallel-1 after double digestion.

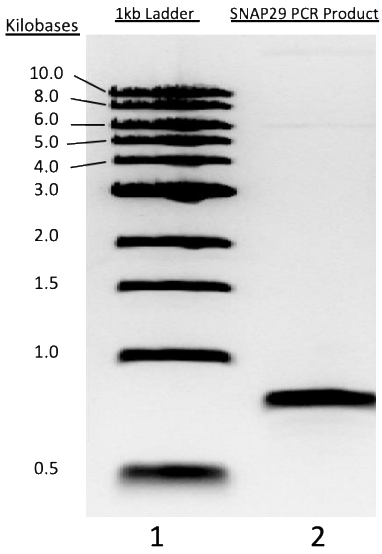

Figure 6: SNAP-29 PCR Product

3.2: Restriction Double Digestion

Following successful PCR amplification and purification of SNAP-29 cDNA, both SNAP-29 and pMBP-parallel-1 were double digested with BamHI and XhoI. Both digested products were then subjected to gel electrophoresis and imaged (Fig. 7). The undigested pMBP-parallel-1 vector shows the typical plasmid banding pattern with three bands corresponding to circularized (band greater than 10 Kb), nicked (band at 7.5 Kb), and supercoiled (band at 5.5 Kb) conformations in lane 2. Upon double digestion, pMBP-parallel-1 produced a single band at 6.7 Kb, which is consistent with the expected size of linearized pMBP-parallel-1 in lane 3. Double digested SNAP-29 shows a band at approximately 0.8 Kb, which is consistent with the expected size of 777 bp for SNAP-29 in lane 4. Because electrophoresis revealed that both pMBP-parallel-1 and SNAP-29 appeared at the expected positions in the gel, these bands were subsequently purified from the gel. Gel purification yielded a concentration of 27.4 ng/µL with absorbance ratios of A260/280 = 1.46 and A260/230 = 1.29 for SNAP-29. The absorbance ratios were well below 2.0, meaning that the DNA sample was contaminated following gel extraction. Gel purification yielded a concentration of 16.8 ng/µL with absorbance values of A260/280 = 1.75 and A260/230 = 0.05 for pMBP-parallel-1 (Table 6). The low A260/230 value indicated that there were residual ethanol and other contaminants that were not removed during extraction. Because this is a common issue with gel extractions, these samples were kept and included in a ligation mixture. The ligation reaction utilized T4 DNA Ligase to insert SNAP-29 into the pMBP-parallel-1 bacterial expression vector. To control for vector self-ligation, two separate ligation reactions were carried out. In the experimental condition, a ligation mixture containing T4 DNA Ligase, Ligase Buffer,

SNAP-29 cDNA, and pMBP-parallel-1 DNA was used. In the vector-only control condition, the purified SNAP-29 cDNA was omitted. These ligation mixtures were subsequently used to transform NovaBlue *E. coli* cells.

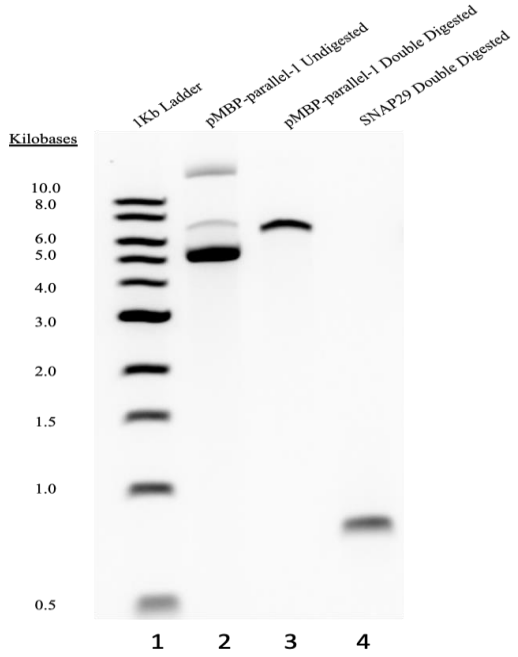

Figure 7: Restriction Digestion Products

Table 6: Gel Purification Results

	Concentration	A260/280	A260/230
SNAP-29	27.4 ng/µL	1.46	1.29
pMBP-parallel-1	16.8ng/µL	1.75	0.05

3.3: Transformation of NovaBlue *E. coli* Cells

Competent NovaBlue *E. coli* cells were transformed with mixtures from the ligation reactions. To control for vector self-ligation, two separate transformation reactions were also carried out. In the experimental condition, the complete ligation mixture was used to transform NovaBlue cells. In the control condition, the vector only control ligation mixture was used to transform NovaBlue cells. Colonies that were formed in the vector only condition correspond to cells that were transformed with pMBP-parallel-1 that reannealed without inclusion of SNAP-29. This control was included to assess the number of false positives that were obtained in the experimental condition. Transformation yielded 136 colonies in the experimental condition and zero colonies in the vector only condition (Fig. 8). Because no insert was included in the vector only condition, a circularized plasmid suitable for *E. coli* transformation was not formed. The absence of transformants observed in this condition indicated that there was minimal reannealing of the vector, meaning that any colonies in the experimental condition likely contained the recombinant plasmid of interest. It was observed that the colonies appear to be closely localized forming indistinct colonies in some instances. It is thought that this was due to uneven spreading of the transformation mixtures on the agar plate while rotating horizontally. To ensure that pure colonies were isolated, two independent colonies were streaked from the experimental plate onto fresh 100 µg/mL Ampicillin LB plates. Pure isolated colonies were then subsequently taken from these plates, inoculated in LB with 100 µg/mL Ampicillin and grown overnight.

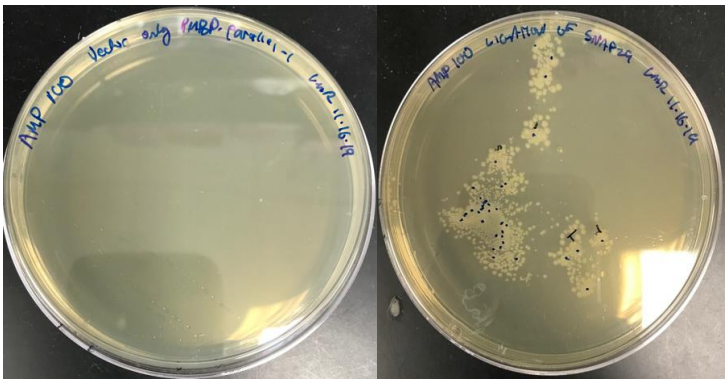

Figure 8: pMBP-parallel-1-SNAP-29 Transformation Plates LB plate with 100 µg/mL Ampicillin and pMBP-parallel-1 only ligation transformation (Left) and LB plate with 100 µg/mL Ampicillin and experimental ligation transformation (Right).

3.4: Isolated Plasmid Screening

Plasmids were isolated from two pure independent colonies that grew from streaked plates. Isolation yielded a DNA concentration of 94.4 ng/µL for isolate #1 and a DNA concentration of 79.5 ng/µL for isolate #2. Both A260/280 and A260/230 absorbance ratios for each isolate were close to 2.0, indicating high sample purity and the absence of both organic and inorganic contaminants (Table 7). These isolates were then double digested with BamHI and XhoI to screen for recombinant plasmids containing SNAP-29. These digests were subsequently separated on a 0.7% agarose gel and imaged (Fig. 9). Colonies containing the plasmid of interest should exhibit bands at approximately 0.8 Kb and 6.7 Kb, corresponding to SNAP-29 and linearized pMBP-parallel-1, respectively. Plasmid screening showed that double digested SNAP-29 isolates #1 and #2 produced bands at approximately 0.8 Kb and 6.7Kb corresponding to SNAP-29 and pMBP-parallel-1. Therefore, both isolates were subsequently sent to Eurofins Genomics for sequencing.

Table 7: Plasmid Isolation Results

	Concentration	A260/280	A260/230
SNAP-29 Isolate #1	94.4 ng/µL	1.86	2.33
SNAP-29 Isolate #2	79.5ng/µL	1.88	2.31

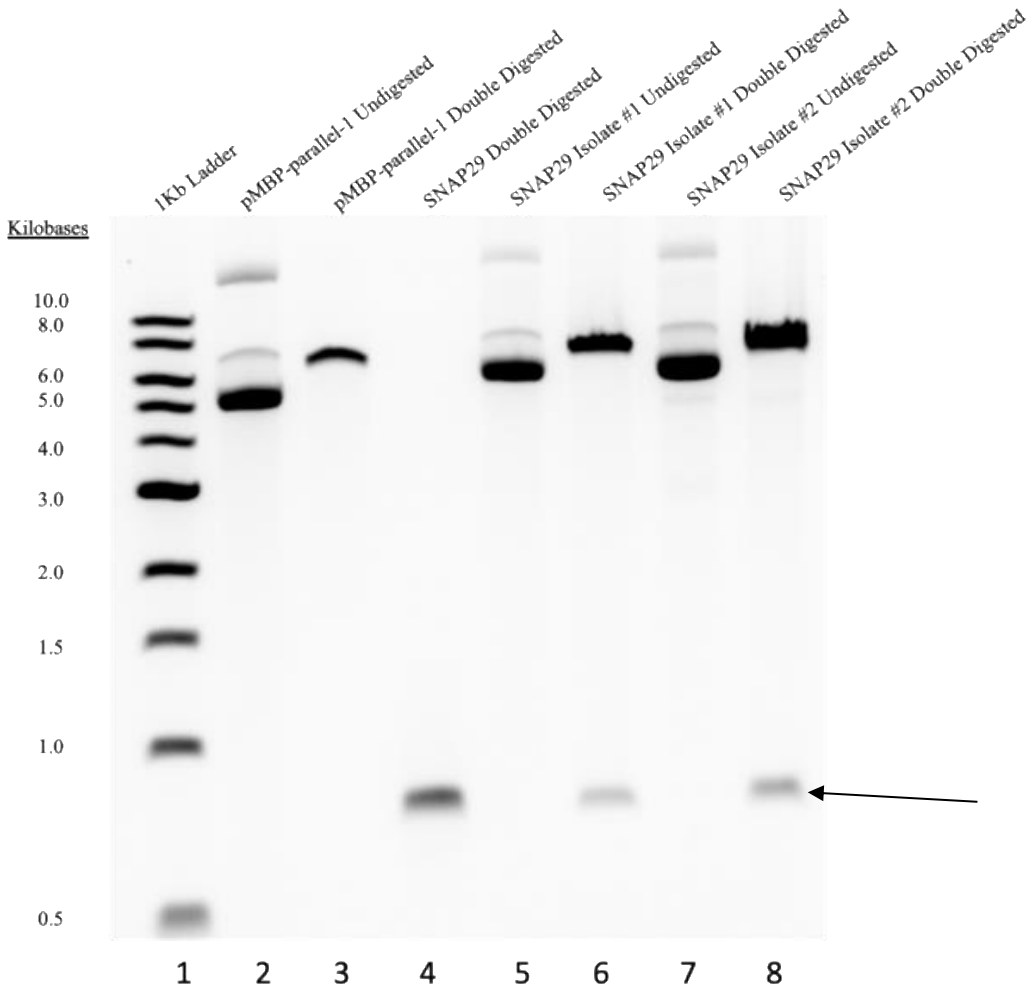

Figure 9: pMBP-parallel-1-SNAP-29 Isolate Screening Lanes 1-4 were represented in Fig. 7. The SNAP-29 band is indicated by an arrow.

3.5: Sequencing Confirmation of Isolated Plasmids

After analysis by restriction digestion, the two plasmid isolates shown in Fig. 9 (lanes 5 and 8) were selected for sequencing with a pMBP forward primer. This primer is complementary to a portion of the MBP sequence within the pMBP-parallel-1 vector (Table 5). The sequencing results for Isolate #1 showed that 1,143 bp of sequence were generated and the results for Isolate #2 indicated that 1,122 bp were generated. These sequences were analyzed using NCBI nBLAST using the expected cDNA obtained from NCBI for SNAP-29 as the query sequence (Fig. 10). These results showed that both isolated plasmids contained regions of 100% identity to the query sequence without gaps or mismatched nucleotides. The start codon is highlighted by a green box while the stop codon is highlighted by a red box in both Figs. 9A and B.

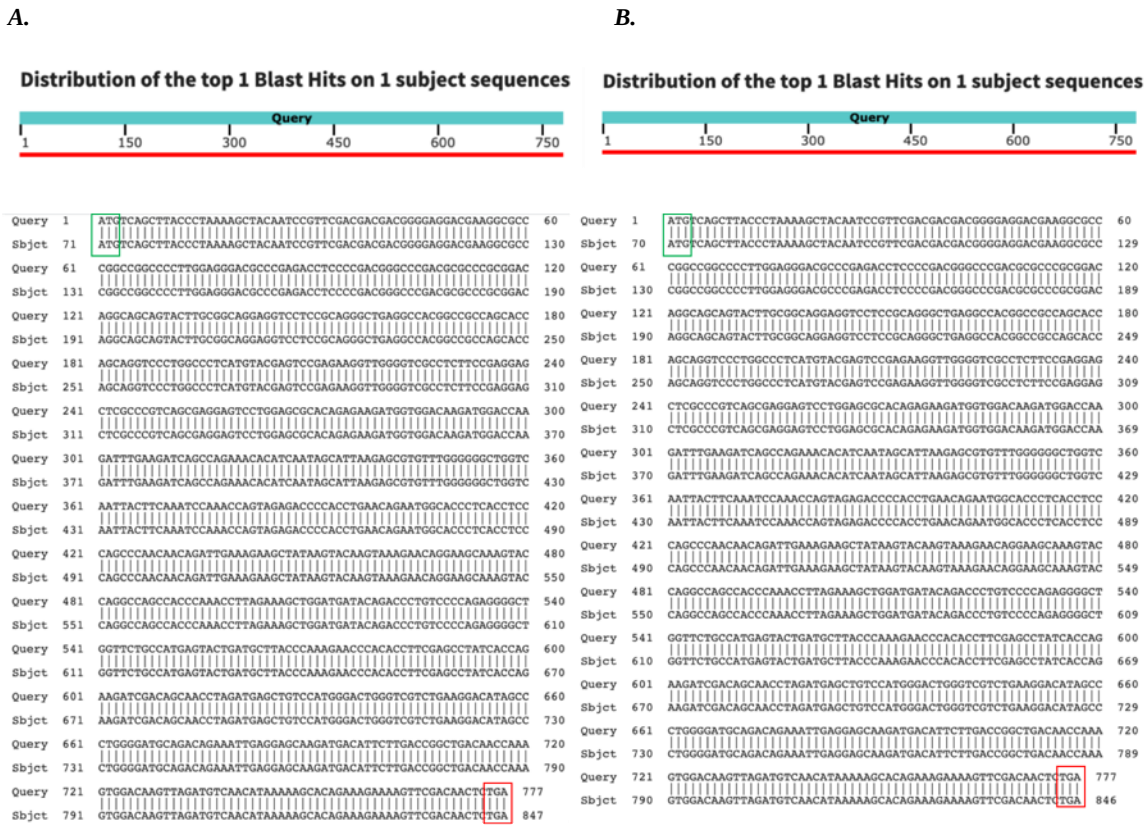

Figure 10: pMBP-parallel-1-SNAP-29 Isolate Sequencing Confirmation SNAP-29 Isolate #1 (A) and SNAP-29 Isolate #2 (B) sequencing data with MBP forward sequencing primer. Both of these figures show 100% similarity, 0 mismatches, and 0 gaps. Green boxes indicate start codons while red boxes indicate stop codons.

The sequences also demonstrated that SNAP-29 was inserted in-frame for both isolated plasmids. This is indicated by the observation that the methionine codon (ATG) of the SNAP-29 cDNA is in frame with the TEV site and with the MBP fusion protein (Fig. 11). These results confirmed that the SNAP-29 cDNA was inserted in frame without any mutations, so the generated constructs were further used to express SNAP-29 in *E. coli*.

A.

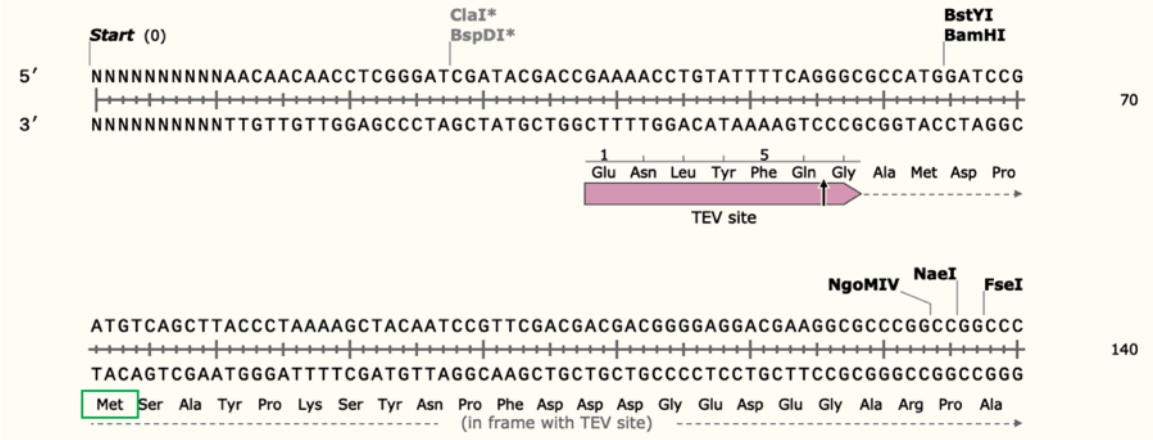

B.

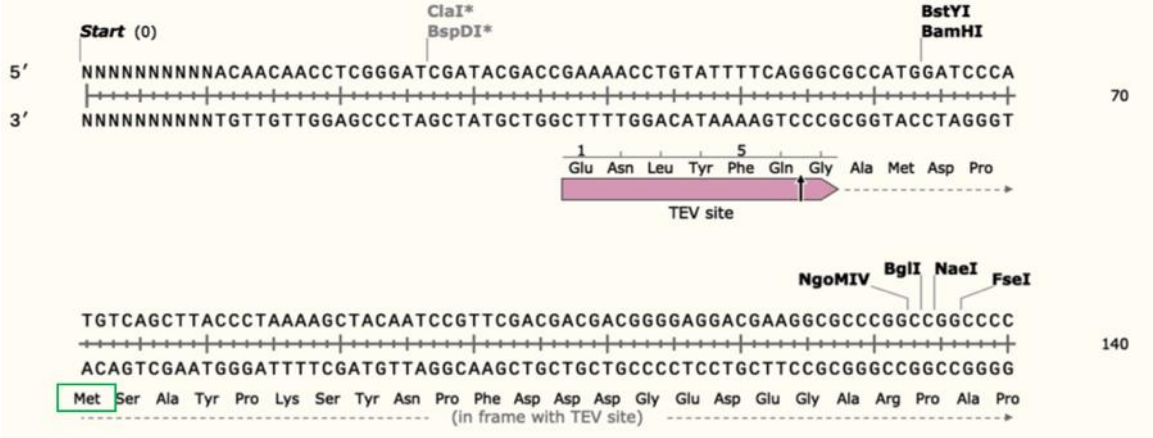

Figure 11: pMBP-parallel-1-SNAP-29 Isolates Confirmed to be In Frame
SNAP-29 Isolate #1 (A) and SNAP-29 Isolate #2 (B) sequencing data with MBP Forward sequencing primer. The ATG start codon from SNAP-29 is indicated by a green box in both A and B.

3.6: SNAP-29 Expression

After both pMBP-parallel-1-SNAP-29 constructs had been confirmed, both constructs were used to transform Rosetta 2 (DE3) *E. coli* cells. This cell line contains the pRare plasmid, which codes for tRNAs that are rarely found in bacteria, allowing for expression of human SNAP-29 without complication due to typical *E. coli* codon usage bias (Novy, Drott, Yaeger, & Mierendorf, 2001). This transformation resulted in the formation of hundreds of colonies for both constructs. Following transformation, a single colony was streaked out from each plate to ensure that a pure colony was obtained. A

single colony from each streak plate was inoculated into LB media containing 34 µg/mL Chloramphenicol and 100 µg/mL Ampicillin and grown in a rotating shaker overnight. The overnight cultures were then induced with IPTG to express SNAP-29. The cells were then lysed and their contents were analyzed via SDS-PAGE. The size of each protein was approximated by comparing the bands in each lane to the bands of known size in the BroadRange Standard. Because SNAP-29 has a known molecular weight of 29 kDa and the fusion protein MBP has a known molecular weight of 42.5 kDa, induction was expected to result in an abundant recombinant polypeptide with a molecular weight of 71.5 kDa. This result is expected as pMBP-parallel-1 codes for the MBP fusion protein along with the inserted SNAP-29. Using the pMBP-parallel-1 vector allowed for the expression of MBP-SNAP29. MBP will serve as a tag which may be used for downstream purification of the protein. The SDS-PAGE results showed that both isolates produced a heavier band in the IPTG (+) condition at 71.5 kDa than in the IPTG (-) condition (Figure 12). This finding, along with the consistent expression of actin (band at 42 kDa) and chloramphenicol acetyltransferase (CAT) (band at 26 kDa) across all conditions indicated that SNAP-29 expression was successfully induced in cells transformed with both SNAP-29 Isolate #1 and SNAP-29 Isolate #2 recombinant plasmids. Actin is abundant in the competent Rosetta 2 (DE3) cells and serves as a marker indicating that cells in all conditions were in the same stage of growth. The CAT protein is encoded by the pRare plasmid which is found in Rosetta 2 (DE3) cells. Constant expression of CAT in all conditions further indicates that these cells were all in the same stage of growth.

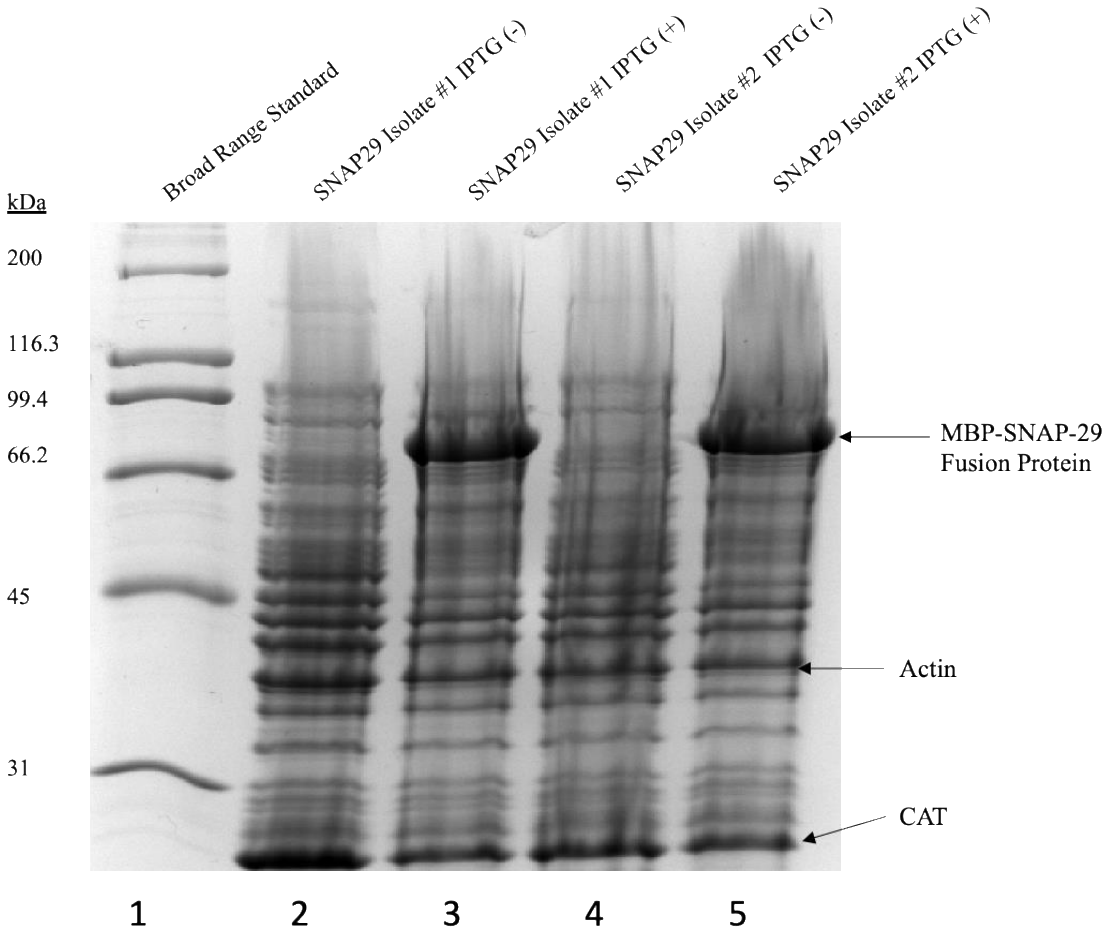

Figure 12: Expression of pMBP-parallel-1-SNAP-29 in Rosetta 2 *E. coli* Cells

Chapter 4: Discussion

The SNAP-29 cDNA was successfully amplified by PCR and inserted into the pMBP-parallel-1 expression vector using restriction digestion and ligation. This construct was confirmed by sequencing and transformed into Rosetta 2 (DE3) *E. coli* cells. These cells were induced with IPTG to express SNAP-29 which was then confirmed by SDS-PAGE analysis.

Further efforts within the Xu lab will be aimed at the large-scale IPTG induced expression of SNAP-29 in Rosetta 2 (DE3) cells that have been transformed with the recombinant human SNAP-29 cDNA. Following this large-scale expression, the bacterial cells will be harvested by centrifugation and suspended in a binding buffer. These cells will then be lysed by a French press technique and centrifuged to remove cellular debris. Next, these samples will be passed through a filter before application to an amylose resin. The MBP-SNAP-29 fusion protein will bind tightly to the amylose resin. This will allow for other proteins that were released from the lysed bacterial cells to be discarded as the resin is washed with additional binding buffer. An eluting buffer containing maltose will then be used to elute the MBP-SNAP-29 fusion protein from the amylose resin. Because MBP has a higher affinity for maltose than amylose, elution will occur readily. The purified SNAP-29 will then be treated with TEV protease to cleave the MBP fusion tag from SNAP-29. Finally, the purified and processed SNAP-29 protein will be used in experiments to decipher its interactions with ORF33/38.

To dissect the functional interactions between SNAP-29 and ORF33/38, lipid mixing assays will be utilized. The purified SNAP-29 protein will be incorporated into artificial autophagosomes along with Qa-SNARE STX-17. These artificial

autophagosomes will then be mixed with artificial lysosomes containing the SNAP-29 cognate SNARE partner, VAMP-8. The autophagosome will contain quenched florescent lipids that will fluoresce upon mixing with lipids from the artificial lysosome. Measuring the degree of florescence over a one-hour period will, thus, measure the degree of fusion that occurs between the two artificial membranes. The KSHV ORF33/38 proteins will also be included in the assays in a range of concentrations to assay how this protein complex affects membrane fusion.

To delineate the structural elements in SNAP-29 that are required for interaction with ORF33/38, a mutational analysis approach will be employed. In these investigations, the wild-type SNAP-29 protein that was expressed in this project will be used in control assays to examine how wild-type SNAP-29 and VAMP-8 membranes are able to fuse in the presence of ORF33/38. Site-directed mutagenesis will then be utilized in order to introduce single amino acid mutations within key SNAP-29 domains in the recombinant plasmid that was produced as a part of this project. Lipid mixing assays will be carried out as described, but mutant SNAP-29 proteins will be utilized. For one phase of this experiment, the SNAP-29 residue Q161 will be replaced by an alanine residue by site-directed mutagenesis. Lipid mixing assays will then be employed to determine if ORF33/38 interacts with SNAP-29 in the same manner as the EV-D68 C3 protein. Further mutants will also be generated by altering the amino acid sequence of SNAP-29's Qa-SNARE domain (75-115) and Qb-SNARE domain (213-258). These mutants will be expressed and utilized in lipid-mixing assays to test ORF33/38 interactions with these domains. The results gleaned from these mutational lipid-mixing assays are anticipated to reveal amino acid substitutions which increase fusion of mutant SNAP-29/wild-type

STX-17 membranes with VAMP-8 membranes in the presence of ORF33/38. Thus, these substituted amino acids could represent sites which could be modulated by drug binding.

Identifying the specific residues involved in the SNAP-29 and ORF33/38 interaction would create a foundation for a novel mechanism by which KSHV infection could be combatted. Pharmaceutical agents could be designed to modulate these amino acids to fortify autophagosome-lysosome binding in mast cells. This approach would allow mast cells to better clear KSHV and would render the cells unable to serve as reservoirs of infection. These drugs could effectively inhibit the long-term perpetuation of KSHV infection and resultant tumor maturation within Kaposi's Sarcoma. This approach, combined with conventional therapies, holds promise to provide a more effective means of treating Kaposi's Sarcoma.

References

Ayers, L. W., Barbachano-Guerrero, A., McAllister, S. C., Ritchie, J. A., Asiago-Reddy, E., Bartlett, L. C., ... & King, C. A. (2018). Mast cell activation and KSHV infection in Kaposi sarcoma. *Clinical Cancer Research*, *24*(20), 5085-5097. DOI: 10.1158/1078-0432.CCR-18-0873

Arora, P., & Ansari, S. H. (2019). Role of various mediators in inflammation of asthmatic airways. In C. Pereira (Ed.), *Asthma-Biological Evidences* (Ch. 7.). IntechOpen. DOI: 10.5772/intechopen.84357

Aoki, R., Kawamura, T., Goshima, F., Ogawa, Y., Nakae, S., Nakao, A., ... & Shimada, S. (2013). Mast cells play a key role in host defense against herpes simplex virus infection through TNF-α and IL-6 production. *Journal of Investigative Dermatology*, *133*(9), 2170-2179. DOI: 10.1038/jid.2013.150

Corona, A. K., Saulsbery, H. M., Velazquez, A. F. C., & Jackson, W. T. (2018). Enteroviruses remodel autophagic trafficking through regulation of host SNARE proteins to promote virus replication and cell exit. *Cell Reports*, *22*(12), 3304-3314. DOI: 10.1016/j.celrep.2018.03.003

Fasshauer, D., Sutton, R. B., Brunger, A. T., & Jahn, R. (1998). Conserved structural features of the synaptic fusion complex: SNARE proteins reclassified as Q-and R-SNAREs. *Proceedings of the National Academy of Sciences of the U.S.A.*, *95*(26), 15781-15786. DOI: 10.1073/pnas.95.26.15781

Ganem, D. (2006). KSHV infection and the pathogenesis of Kaposi's sarcoma. *Annual Review of Pathology: Mechanisms of Disease*, *1*, 273-296. DOI: 10.1146/annurev.pathol.1.110304.100133

Gilfillan, A. M., & Beaven, M. A. (2011). Regulation of mast cell responses in health and disease. *Critical Reviews™ in Immunology, 31*(6), *475–529.* DOI: 10.1615/CritRevImmunol.v31.i6.30

Grundhoff, A., & Ganem, D. (2004). Inefficient establishment of KSHV latency suggests an additional role for continued lytic replication in Kaposi sarcoma pathogenesis. *The Journal of Clinical Investigation*, *113*(1), 124-136. DOI: 10.1172/JCI17803

Karanasios E., Ktistakis N.T. (2016) Signalling in Autophagy. In Autophagy at the Cell, Tissue and Organismal Level. *SpringerBriefs in Cell Biology*,17-33. DOI: 10.1007/978-3-319-33145-4

Kloepper, T. H., Kienle, C. N., & Fasshauer, D. (2007). An elaborate classification of SNARE proteins sheds light on the conservation of the eukaryotic endomembrane system. *Molecular Biology of the Cell*, *18*(9), 3463-3471. DOI: 10.1091/mbc.e07-03-0193

Kraft, S., & Kinet, J. P. (2007). New developments in FcεRI regulation, function and inhibition. *Nature Reviews Immunology*, *7*(5), 365-378. DOI: 10.1038/nri2072

Lei, Y., Gregory, J. A., Nilsson, G. P., & Adner, M. (2013). Insights into mast cell functions in asthma using mouse models. *Pulmonary Pharmacology & Therapeutics*, *26*(5), 532-539. DOI: 10.1016/j.pupt.2013.03.019

Levine, B. (2005). Eating oneself and uninvited guests: autophagy-related pathways in cellular defense. *Cell*, *120*(2), 159-162. DOI: 10.1016/j.cell.2005.01.005

Lorentz, A., Baumann, A., Vitte, J., & Blank, U. (2012). The SNARE machinery in mast cell secretion. *Frontiers in Immunology*, *3*, 143. DOI: 10.3389/fimmu.2012.00143

Moon, T. C., St Laurent, C. D., Morris, K. E., Marcet, C., Yoshimura, T., Sekar, Y., & Befus, A. D. (2010). Advances in mast cell biology: new understanding of heterogeneity and function. *Mucosal Immunology*, *3*(2), 111-128. DOI: 10.1038/mi.2009.136

Nishida, K., Yamasaki, S., Ito, Y., Kabu, K., Hattori, K., Tezuka, T., ... & Yamamoto, T. (2005). FcεRI-mediated mast cell degranulation requires calcium-independent microtubule-dependent translocation of granules to the plasma membrane. *The Journal of Cell Biology*, *170*(1), 115-126. DOI: 10.1083/jcb.200501111

Novy, R., Drott, D., Yaeger, K., & Mierendorf, R. (2001). Overcoming the codon bias of *E. coli* for enhanced protein expression. *Innovations*, *12*, 1-3.

Piliponsky, A. M., Chen, C. C., Rios, E. J., Treuting, P. M., Lahiri, A., Abrink, M., ... & Galli, S. J. (2012). The chymase mouse mast cell protease 4 degrades TNF, limits inflammation, and promotes survival in a model of sepsis. *The American Journal of Pathology*, *181*(3), 875-886. DOI: 10.1016/j.ajpath.2012.05.013

Richards, A. L., & Jackson, W. T. (2012). Intracellular vesicle acidification promotes maturation of infectious poliovirus particles. *PLoS Pathogens*, *8*(11). DOI: 10.1371/journal.ppat.1003046

Shelburne, C. P., & Abraham, S. N. (2011). The mast cell in innate and adaptive immunity. *Mast Cell Biology*, *716*, 162-185. DOI: 10.1007/978-1-4419-9533-9_10

Takáts, S., Glatz, G., Szenci, G., Boda, A., Horváth, G. V., Hegedűs, K., ... & Juhász, G. (2018). Non-canonical role of the SNARE protein Ykt6 in autophagosome-lysosome fusion. *PLoS Genetics*, *14*(4). DOI: 10.1371/journal.pgen.1007359

Toonen, R. F., Kochubey, O., de Wit, H., Gulyas-Kovacs, A., Konijnenburg, B., Sørensen, J. B., ... & Verhage, M. (2006). Dissecting docking and tethering of secretory vesicles at the target membrane. *The EMBO Journal*, 25(16), 3725-3737. DOI: 10.1038/sj.emboj.7601256

Urb, M., & Sheppard, D. C. (2012). The role of mast cells in the defence against pathogens. *PLoS Pathogens*, *8*(4). DOI: 10.1371/journal.ppat.1002619

Waern, I., Karlsson, I., Thorpe, M., Schlenner, S. M., Feyerabend, T. B., Rodewald, H. R., ... & Wernersson, S. (2012). Mast cells limit extracellular levels of IL-13 via a serglycin proteoglycan-serine protease axis. *Biological Chemistry*, *393*(12), 1555-1567. DOI: 10.1515/hsz-2012-0189

Wu, J. J., Avey, D., Li, W., Gillen, J., Fu, B., Miley, W., ... & Zhu, F. (2016). ORF33 and ORF38 of Kaposi's sarcoma-associated herpesvirus interact and are required for optimal production of infectious progeny viruses. *Journal of Virology*, *90*(4), 1741-1756. DOI: 10.1128/JVI.02738-15

Xu, H., Bin, N. R., & Sugita, S. (2018). Diverse exocytic pathways for mast cell mediators. *Biochemical Society Transactions*, 46(2), 235-247. DOI: 10.1042/BST20170450